ASYMPTOTIC DYNAMICS OF THE SLOW-FAST HINDMARSH-ROSE NEURONAL SYSTEM

Nathalie Corson[1] and M.A. Aziz-Alaoui[1]

[1]Laboratoire de Mathématiques Appliquées du Havre
25 rue Philippe Lebon, 76600 Le Havre, France

Corresponding author email: nathalie.corson@univ-lehavre.fr

Abstract. This work adresses the asymptotic dynamics of a neuronal mathematical model. The aim is first the understanding of the biological meaning of existing mathematical systems concerning neurons such as Hodgkin-Huxley or Hindmarsh-Rose models. The local stability and the numerical asymptotic analysis of Hindmarsh-Rose model are then developed in order to comprehend bifurcations and dynamics evolution of a single Hindmarsh-Rose neuron. This has been performed using numerical tools borrowed from the nonlinear dynamical system theory.

Keywords. neuron model, asymptotic dynamics, bifurcation, chaos.

AMS (MOS) subject classification: 34C15, 37D45, 37G35, 37N25, 65P20, 92C20.

1 Introduction and neurophysiology

Also called *nerve cells*, *neurons* are the most important cells of the nervous system. They are composed of a cell body, or soma, extended by an axon, an axon terminal and some dendrites (Fig. 1). These extensions are useful not only for the transmission of information through a neuron but also for the transmission from a neuron to another. Connections between neurons are possible thanks to synapses.
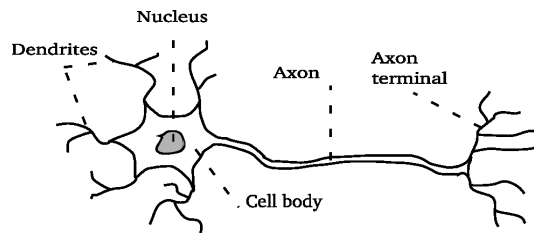

Figure 1: Structure of a typical neuron.

Ionic channels can be seen as macrocellular pores in the neuron membrane. They enable molecules to pass through the membrane. They are the link between intra-cellular and extra-cellular space. There are many types of ionic channels. For example, we may cite those which are always open, those which are voltage-dependent or those which select the molecule allowed to cross the membrane. *Sodium channels* are so called because they are specific to sodium ions. They can be in an active state or in an inactive one. *Potassium channels* open and close with delay. *Leak channel* are always open.

Neurons are enclosed by a membrane which separates the interior of the cell from the extracellular space. On the inside of the cell, the concentration of ions is different than in the surrounding liquid. The difference of concentration generates an electrical potential which plays an important role in neuronal dynamics. The last is the *membrane potential*.

When not sending any signal, a neuron is *at rest*. At rest, there are relatively more sodium ions (Na+) on the outside of the neuron and more potassium (K+) ions on the inside. The inside of the neuron is negative compared to the outside. The difference in the voltage between the inside and the outside of the neuron gives the *resting potential*, the value of which is in general about -70 mV.

The *equilibrium potential* is predictable with the Nernst equation. It is given by, $E(S) = \dfrac{RT}{ZF} ln \dfrac{[S]_{out}}{[S]_{in}}$, where $E(S)$ represents the Nernst potential for ion S (measured as for membrane potential, inside with respect to outside), $[S]_{out}$ represents the concentration of S outside the cell, $[S]_{in}$ the concentration of S inside the cell, R is the gas constant, T represents the absolute temperature, Z represents the valence of ion S : $Z(K+) = +1$, $Z(Na+) = -1$, and F is Faraday's constant.

An *action potential*, also called *spike* or *impulse* (Fig. 2) occurs when a neuron sends information along an axon away from the cell body. The action potential is an explosion of electrical activity that is created by a depolarizing current. A stimulus makes the resting potential move up towards positive values. If the potential reaches a certain *threshold* (about -55 mV), the neuron fires an action potential the amplitude of which is always the same. If the potential does not reach this threshold value, no action potential fires. Therefore, a neuron respects the *all or none* principle.
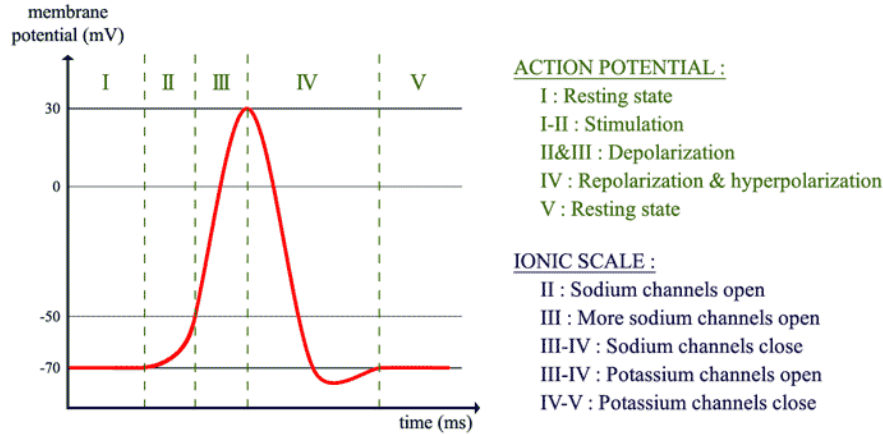
Figure 2: Action potential (spike or impulse).

Action potentials are caused by an exchange of ions across the neuron membrane. When a stimulus is applied, sodium channels open. Since there is much more sodium ions on the outside of the neuron and since the inside of the neuron is negative compared to the outside, sodium ions rush into the neuron. As sodium has a positive charge, the neuron becomes more positive, that is *depolarized*. Besides, potassium channels open with delay. When they do open, potassium goes out of the cell, reversing the depolarization. At that time, sodium channels start to close. This induces the *repolarization*. Indeed, it makes the membrane potential go back towards the resting potential. Then, there is the *hyperpolarization* of the neuron, since the potential goes past the resting potential because the potassium channels close with delay. Gradually, the ion concentrations go back to resting levels and the cell returns to -70 mV (Fig. 2). For more details, see for example [7].

A *burst* is a group of at least two action potentials that occur close together in time, separated from other action potentials by large time intervals which are called *quiescent* or *silent phases*.
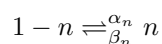
2   Mathematical models

Two neurophysiologists, *Alan Lloyd Hodgkin* and *Andrew Fielding Huxley*, have developed an empirical kinetic description of ionic mechanisms in a neuron, see [10]. This description was not only simple enough to make practical computation of electrical responses but also sufficiently precise so as to predict conduction and major features of excitability. Their model comprises mathematical equations and suggests the main behaviour of the gating mechanisms, [7,10]. For shortness, *HH* is a reference to the Hodgkin Huxley model.

The model is based on Sodium, Potassium and leakage ion flow. *HH* model has separated equations for sodium conductance g_{Na} and potassium conductance g_K. They are expressed as maximum conductances $\bar{g}_{Na}$ and $\bar{g}_K$ multiplied by coefficients representing the fraction of the maximum conductances actually expressed. The multiplying coefficients are numbers varying between 0 and 1. In the model, the conductance changes depend only on voltage and time. Because of their observations, Hodgkin and Huxley noted that such kinetics would be obtained if the opening of a K channel is controlled by several independent "particles". Suppose that there are four identical particles, each one with a probability n of being in the correct position to set up an open channel. The probability that all four particles are correctly placed is n^4.

Mathematically, I_K is represented in the *HH* model by,

$$I_K = n^4 \bar{g}_K (V - E(K))$$

The voltage and time dependent changes of n are given by the reaction,

$$1 - n \underset{\beta_n}{\overset{\alpha_n}{\rightleftharpoons}} n$$

where the gating particles make transitions between the permissive and non-permissive forms with voltage-dependent rate constants α_n and β_n. If the initial value of the probability n is known, subsequent values can be computed by solving the simple differential equation,

$$\frac{dn}{dt} = \alpha_n(1 - n) - \beta_n n$$

The *HH* model uses a similar formalism to describe I_{Na}, with four hypothetical gating particles making independent first order transitions between permissive and non permissive state to control the channel. However, because there are two opposing gating processes, activation and inactivation, there must be two kinds of gating particles, say h and m. Three m particles control activation and one h particle controls inactivation. Therefore, the probability that they are all in permissive position is $m^3 h$. I_{Na} is then represented by,

$$I_{Na} = m^3 h \bar{g}_{Na} (V - E(Na))$$

As for the n parameter of K channels, m and h are assumed to undergo transitions between permissive and non-permissive forms with rates satisfying differential equations,

$$\frac{dm}{dt} = \alpha_m(1 - m) - \beta_m m$$

$$\frac{dh}{dt} = \alpha_h(1 - h) - \beta_h h$$

HH model for the squid giant axon describes ionic current accross the membrane in terms of three components,

$$I_{Na} = m^3 h \bar{g}_{Na}(V - E(Na)) \ , \quad I_K = n^4 \bar{g}_K(V - E(K)) \ , \quad I_L = \bar{g}_L(V - E(L))$$

where $\bar{g}_L$ is a fixed background leakage conductance.

Therefore, the HH model reads as follows,

$$\begin{cases} -C \dfrac{dV}{dt} &= m^3 h \bar{g}_{Na}(V - E(Na)) + n^4 \bar{g}_K(V - E(K)) + \bar{g}_L(V - E(L)) - I \\ \dfrac{dn}{dt} &= \alpha_n(1 - n) - \beta_n n \\ \dfrac{dm}{dt} &= \alpha_m(1 - m) - \beta_m m \\ \dfrac{dh}{dt} &= \alpha_h(1 - h) - \beta_h h \end{cases}$$

in which C represents the membrane capacity, V the total membrane potential, m the Na activation variable, h the Na inactivation variable, $\bar{g}_{Na}$ the maximum sodium conductance, $E(Na)$ the Na equilibrium potential, n the K activation variable, $\bar{g}_K$ the maximum potassium conductance, $E(K)$ the K equilibrium potential, $\bar{g}_L$ the maximum leakage conductance, $E(L)$ the leakage equilibrium potential, I the external current (applied during an experiment), α_i the gate inactivation rate ($i = m, n, h$), β_i the gate activation rate ($i = m, n, h$).

In 1982, *J.L. Hindmarsh* and *R.M. Rose* simplified the Hodgkin-Huxley model, see [8]. The model they obtained is of Fitzhugh-Nagumo type. Indeed, they observed that some variables could be replaced by constants and they found relations between different variables. Therefore, they simplified the Hodgkin-Huxley system into a more simple one with two euqations, as follows,

$$\begin{cases} \dot{x} = y + ax^2 - x^3 \\ \dot{y} = 1 - dx^2 - y \end{cases} \tag{1}$$

Two years later, Hindmarsh and Rose decided to add a third equation to their model, so that the motion of their model could be closer to the motion of a real neuron, see [9]. This Hindmarsh-Rose model (HR) describes the dynamics of the membrane potential x in the axon of a neuron. It is a three dimensional system of non linear first order differential equations, which reads as,

$$\begin{cases} \dot{x} &= y + ax^2 - x^3 - z + I \\ \dot{y} &= 1 - dx^2 - y \\ \dot{z} &= \epsilon(b(x - x_c) - z) \end{cases} \tag{2}$$

While x describes the membrane potential, y describes the exchange of ions accross the neuron membrane through fast ionic channels and z the exchange of ions through slow ionic channels. Parameters a, b, d are constants experimentally determined and $x_c = -\frac{1}{2}(1 + \sqrt{5})$ is the equilibrium x-coordinate of system (1) for the following parameters,

$$a = 3, \quad b = 4, \quad d = 5, \quad x_c = -\frac{1}{2}(1 + \sqrt{5}) \tag{3}$$

In this paper, I and ϵ are chosen as bifurcation parameters due to their biological meaning. Indeed, I is the applied current while ϵ is a recovery variable, which is very small. This last parameter controls the slow motion of the neuron activity.

This system, as well as HH model, has been studied in different ways, see for example [3,12] or [4,13,14] and the references therein cited. Interesting studies are also presented in [1,2,5,6,11].

3 Bifurcations and Chaos

3.1 Dissipativity and existence of attractors

Theorem 1 *If* $0 < a < \sqrt{3}(1 + \epsilon)^{\frac{1}{2}}$ *then system (2) is dissipative.*

Proof :
The variation of the volume $V(t)$ of a small element $\delta\Omega(t) = \delta x \delta y \delta z$ in the phase space is determined by the divergence of the flow,

$$\nabla V = \frac{\partial \dot{x}}{\partial x} + \frac{\partial \dot{y}}{\partial y} + \frac{\partial \dot{z}}{\partial z}$$

System (2) leads to,

$$\nabla V = -3x^2 + 2ax - 1 - \epsilon$$

$$\nabla V < 0 \Leftrightarrow -3x^2 + 2ax - 1 - \epsilon < 0$$

Therefore, if $-3x^2 + 2ax - 1 - \epsilon < 0$, then $\nabla V < 0$. So that with $0 < a < \sqrt{3}(1 + \epsilon)^{\frac{1}{2}}$, system (2) is dissipative (obviously, one can prove the existence of a larger parameters range for which this system remains dissipative).

$\square$

Besides, since $-3x^2 + 2ax - 1 - \epsilon < \frac{a^2}{3} - 1 - \epsilon < 0$, system (2) has, for the volume element $\delta\Omega(t) = \delta x \delta y \delta z$, an exponential contraction rate satisfying,

$$\delta\Omega(t) \le e^{\frac{a^2}{3} - 1 - \epsilon},$$

That is, a volume element V_0 is contracted by the flow into a volume element less than $V_0 e^{(\frac{a^2}{3}-1-\epsilon)t}$ in time t. In other words, each volume containing the system trajectory shrinks to zero as $t \to \infty$ at an expontential rate less than $\frac{a^2}{3} - 1 - \epsilon$, which is independent of x, y and z. Thus, all trajectories are ultimately confined to a specific subset having zero volume (which, of course, can not ensure the existence of bounded attractor), this has been confirmed by our computer simulations.

The chaotic behaviour of the Hindmarsh-Rose system is shown by numerical analysis in different regions of the parameters space, by bifurcation diagrams, Lorenz plots, Lyapunov exponents, time series and phase portraits. Since $\epsilon << 1$, the first two equations of HR system correspond to the fast dynamics while the last equation controls the slow dynamics. In figure 3 (e), the fast dynamics is the spiking part of time series while slow dynamics is the resting part. In figure 3 (a), (b), (c), (d), the fast dynamics corresponds to the right part of the attractor, the part where we observe spirals, while slow dynamics is on the left of the figures.
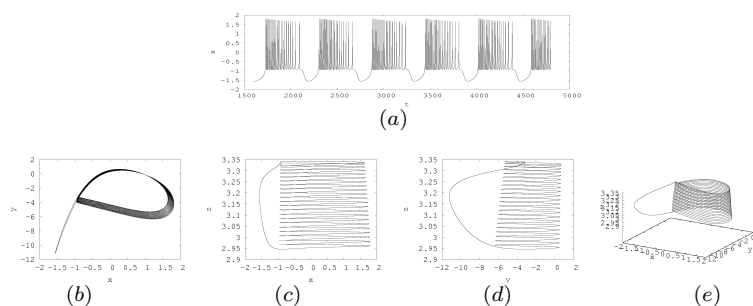

Figure 3: Numerical integration of system (2) for parameters given in (3) with $I = 3.25$ and $\epsilon = 0.001$. (a) : (t,x) times series showing a sequence of action potentials. (b), (c), (d), (e) : phase portraits respectively in x-y projection, x-z projection, y-z projection and (x, y, z) tridimensional view.

An important phenomenon in neuron activity is the transition between spiking and bursting. *Spiking* is represented by a generation of action potentials, while *bursting* is represented by a membrane potential changing from resting to repetitive firing state. We can see also these phenomena looking at time series and phase portraits, but bifurcation diagrams that are shown in this section do not give any information on this "slow-fast" motion. Indeed, in order to obtain these bifurcation diagrams, the chosen Poincaré section crosses the phase portrait within the hole of the attractor which is on the right part on figures 3 *(b,c,d,e)* and corresponds to the fast dynamics. Therefore, the following diagrams give only information about the fast dynamics of HR system.

In the case of neuron dynamics, the location of bifurcation values is impor-

tant to determine the transition between a quiescent state and an oscillatory one, and also between different kinds of oscillatory motion. Therefore, a bifurcation corresponds to a qualitative change of the information transmitted through the axon of the neuron.

In this paper, codimension-1 bifurcations (that is the number of independent conditions determining this bifurcation is one) are numerically computed. We firstly make the slow parameter ϵ be the control parameter and then, the injected current I is chosen for this assignment.

3.2   Dynamics with respect to ϵ

Parameter ϵ is the ratio of time scales between spiking (fast dynamics) and resting (slow dynamics). Therefore, it controls the difference between the slow and the fast dynamics of HR model corresponding to the difference between fast fluxes of ions accross the membrane to slow ones. Thereby, making this parameter evolving to observe the neuron reaction is really interesting, see [4].

A bifurcations diagram show the evolution of the aysmptotic behaviour of solutions according to one parameter.

The successive local maxima map (first return map, Lorenz plot) is a reliable numerical method that gives information about the presence (or not) of chaos for some fixed parameters. This map gives the local maxima of z against the immediatly preceding local maxima. Looking at phase portraits, it is justified to wonder if, for some parameters, HR model exhibits a chaotic dynamics. The Lorenz plot gives a good idea of this possible chaotic behaviour, when the resulting plot is unimodal with a shape similar to a skewed Hénon map. Lyapunov exponents measure the sensibility to initial conditions and are numerical tools to have an idea of the presence of chaos. If all Lyapunov exponents are negative, two initialy close trajectories remain close to each other, while a positive Lyapunov exponent means that two initialy close trajectories diverge. Therefore, plotting the larger Lyapunov exponent gives a reliable evidence of the presence of chaos.

Figure $4(a)$ gives the bifurcation diagram with respect to the control parameter ϵ in the range $[0, 0.05]$. In order to have a more accurate analysis of the dynamics of system (2), we present in figure $4(b),(c),(d)$ enlargements of figure $4(a)$. Figure $4(b)$ shows, among other things, that there is an $\epsilon_1 \in [0.00041, 0.00049]$ for which the neuron behaviour changes abruptly. Indeed, $\forall \epsilon < \epsilon_1$, the neuron exhibits a tonic spiking motion and, $\forall \epsilon > \epsilon_1$, the neuron exhibits a bursting motion. Moreover, this figure shows that system (2) with parameters given in (3) and $I = 3.25$ does not exhibit chaotic behaviour for $\epsilon \in [\epsilon_1, 0.002]$. On figure $5(a)$ one can see that this model does not exhibit any chaotic behaviour for $\epsilon = 0.0005$. Figure $5(b)$ confirms the fact that there is no presence of chaos for $\epsilon \in [\epsilon_1, 0.002]$, since the larger

Lyapunov exponent remains really close to zero. Time series and (x, y, z) phase portraits of figure 6 show how the variation of parameter ϵ makes the dynamics of system (2) change from spiking to periodical bursting. These figures confirm the non-chaotic behaviour of this system for $\epsilon \in [\epsilon_1, 0.002]$. The enlargement of figure 4(a) for $\epsilon \in [0.005, 0.015]$ shown in figure 4(c) exhibits not only inverse period doubling cascades starting with period 3, period 4 or period 5 but also some dark parts, which is a numerical sign of chaotic motion. Some other numerical evidence can be seen, for $\epsilon = 0.008$, on the Lorenz plot of figure 7(a) which gives a typical unimodal map corresponding to a chaotic behaviour. Moreover, either the positive larger Lyapunov exponent of figure 7(b) or the time series and (x, y, z) phase portraits of figure 8 point out the chaotic behaviour of the model for some ranges of $\epsilon \in [0.005, 0015]$.

The enlargement of figure 4(c) for $\epsilon \in [0.0138, 0.0148]$ shown in figure 4(d) also exhibits a chaotic behaviour of system (2). This is confirmed not only by the Lorenz plot for $\epsilon = 0.0145$ (figure 9(a)) but also by the positive larger Lyapunov exponent in the left part of figure 9(b) and by the time series and (x, y, z) phase portrait presented in figure 10($a_{1,2}$).

The right part of figure 4(a) exhibits a reverse period doubling cascade. As ϵ becomes larger, the number of spikes within a burst decreases until the bursting motion of the neuron disappears to let the spiking motion arise. This phenomenum is also obvious while looking at figure 10($b_{1,2}$),($c_{1,2}$),($d_{1,2}$).
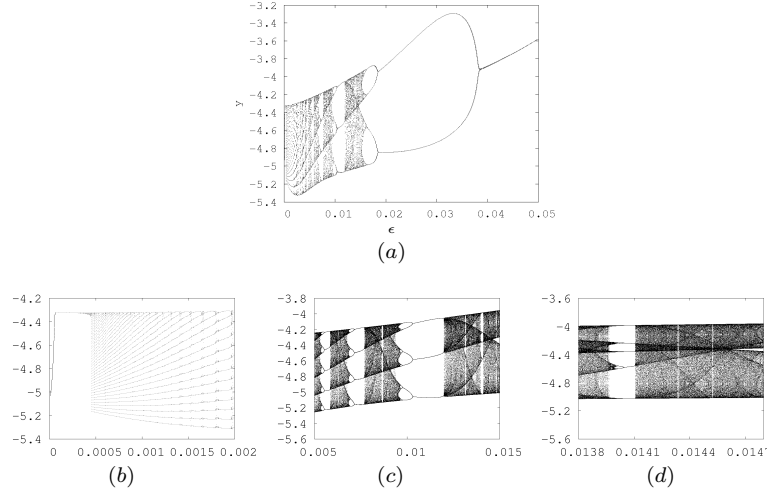

Figure 4: Bifurcation diagrams in (ϵ, y) plane for system (2) with parameters given in (3) and with $I = 3.25$. (a) An inverse period doubling cascade is observed for $\epsilon \in [0, 0.05]$. (b) Enlargement of figure (a) for $\epsilon \in \,]0; 0.002]$. ($c$) Enlargement of figure (a) for $\epsilon \in [0.005; 0.015]$. ($d$) Enlargement of figure (c) for $\epsilon \in [0.0138; 0.0147]$.
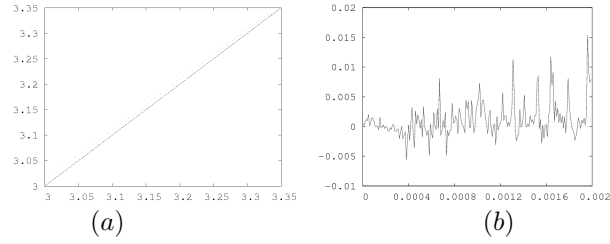
$$(a) \hspace{6cm} (b)$$

Figure 5: System (2) with parameters given in (3) and $I = 3.25$. (a) Successive local maxima in z (i.e. 'Lorenz plot') of the HR model with parameter given in (3), $I = 3.25$ and $\epsilon = 0.0005$. Since this Lorenz plot has not the classical shape of unimodal chaotic map, for these parameters, HR model does not exhibit chaotic motion, (b) Larger Lyapunov exponent which is numerically close to zero for $\epsilon \in [0; 0.002]$. Indeed, for $\epsilon \approx 0.0005$, the larger Lyapunov exponent is close to zero.
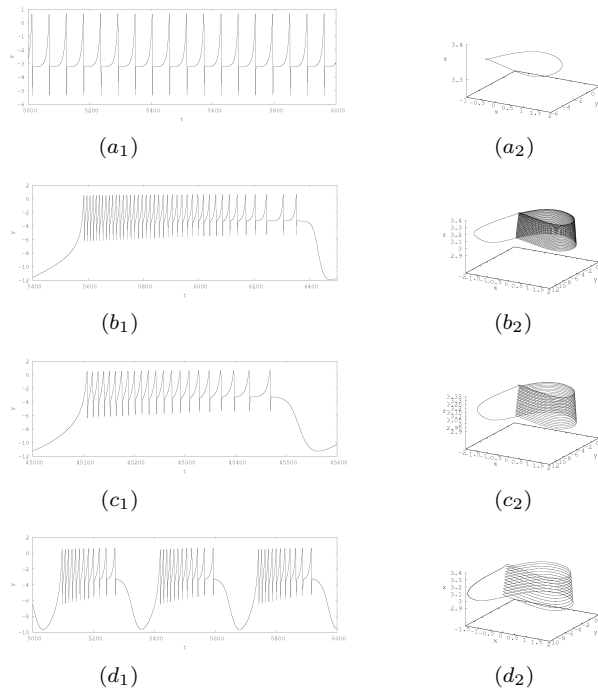

$$(a_1) \hspace{5cm} (a_2)$$

$$(b_1) \hspace{5cm} (b_2)$$

$$(c_1) \hspace{5cm} (c_2)$$

$$(d_1) \hspace{5cm} (d_2)$$

Figure 6: Time series and (x, y, z) phase portraits of system (2) with parameters given in (3) and $I = 3.25$ for (a_1, a_2) $\epsilon = 0.0002$, $(b_1, b2)$ $\epsilon = 0.0005$, (c_1, c_2) $\epsilon = 0.001$, (d_1, d_2) $\epsilon = 0.002$. According to the chosen parameter ϵ, the neuron behaviour changes from tonic spiking (a_1, a_2) to bursting $((b1, b_2)$, (c_1, c_2), $(d_1, d_2))$.

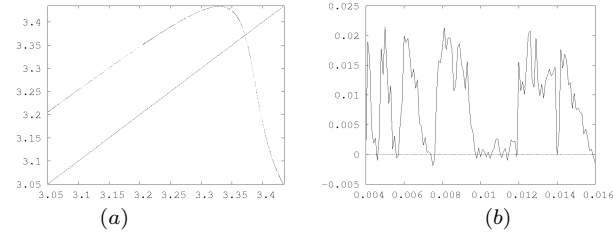(a)   (b)

Figure 7: System (2) with parameter given in (3) and $I = 3.25$. (a) Successive local maxima in z (i.e. 'Lorenz plot') for $\epsilon = 0.008$. It produces a typical tent first-return map, which is a numerical signature of chaos. (b) Larger Lyapunov exponent for $\epsilon \in [0.004; 0.016]$.
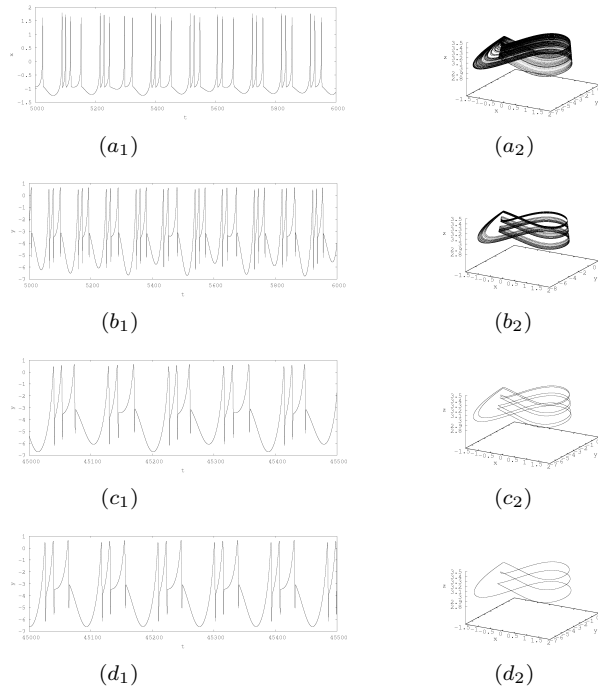

(a_1) (a_2)

(b_1) (b_2)

(c_1) (c_2)

(d_1) (d_2)

Figure 8: Time series and (x, y, z) phase portraits of system (2) with parameters given in (3) and with $I = 3.25$, for (a_1, a_2) $\epsilon = 0.008$, (b_1, b_2) $\epsilon = 0.0095$, (c_1, c_2) $\epsilon = 0.01$, (d_1, d_2) $\epsilon = 0.011$. We observe a period doubling cascade starting with a period three solution.

<center>(a)   (b)</center>
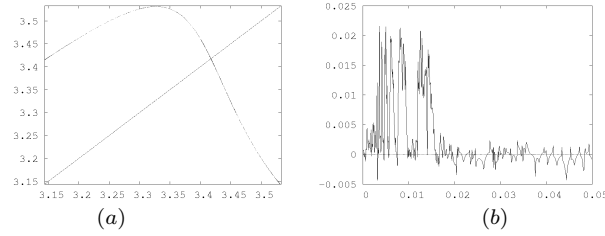
Figure 9: System (2) with parameters given in (3) and $I = 3.25$. (a) First return map to maxima in z for $\epsilon = 0.0145$. It produces a typical tent first-return map, which is a chaos numerical signature, (b) Larger Lyapunov exponent for $\epsilon \in [0; 0.05]$. Since it is positive for $\epsilon = 0.0145$, it also confirms numerically the presence of chaos for these values of parameters.
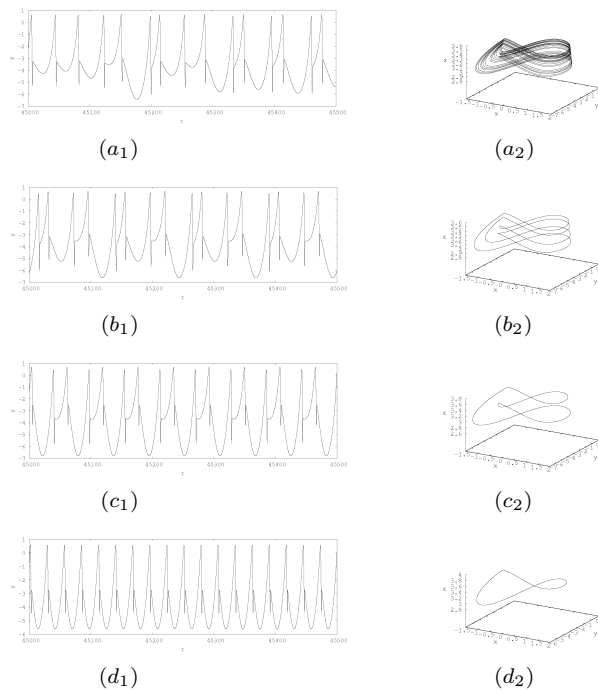

<center>(a_1)   (a_2)</center>

<center>(b_1)   (b_2)</center>

<center>(c_1)   (c_2)</center>

<center>(d_1)   (d_2)</center>

Figure 10: Phase portraits illustrating the bursting bifurcation phenomena in the *HR* model with parameters given in (3) and $I = 3.25$. (a_1, a_2) $\epsilon = 0.0145$, (b_1, b_2) $\epsilon = 0.017$, (c_1, c_2) $\epsilon = 0.03$, (d_1, d_2) $\epsilon = 0.05$. As this slow parameter increases, the period, which corresponds to the number of spikes per burst, decreases. A classical period doubling cascade is observed.

3.3   Dynamics with respect to I

Parameter I corresponds to the current which is injected in the neuron. Thus, it can be controlled during experiments and can then play the role of bifurcation parameter.

Figure 11(a) shows the bifurcation diagram according to the bifurcation parameter I for $I \in [1.25, 4]$ while figure 11(b) is an enlargement of figure 11(a) for $I \in [3.25, 3.3]$. Figure 12(a) shows that the motion of this system is not chaotic for $I = 3.25$. This observation is confirmed by the larger Lyapunov exponent presented in figure 12(b) which remains close to zero for $I \in [3, 3.5]$. Time series and phase portraits given in figure 13 show a periodic behaviour of system (2) for the chosen values of parameter I. Moreover, for each value of I, there is the same number of branches within the bifurcation diagram (figure 11), the same number of spikes within bursts in time series and the same number of laps in the phase portraits (figure 13). This number correponds to the period of the associated limit cycle.
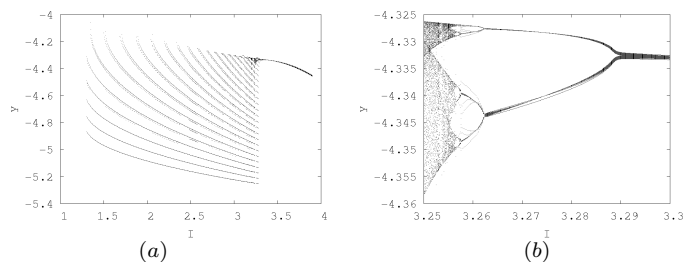

<div align="center">(a)   (b)</div>

Figure 11: (a) Bifurcation diagram of the HR model for parameters (3) and $\epsilon = 0.001$. As the magnitude of injected current I increases, the number of branches on the diagram also increases. Biologicaly, the fast dynamics of the neuron is evolving. (b) Enlargements of (a) for $I \in [3.25; 3.3]$.

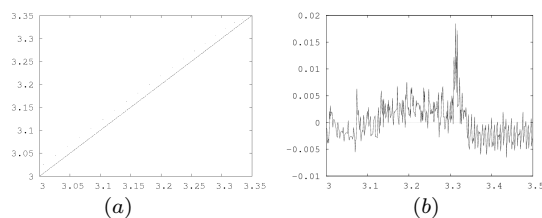<div align="center">(a)   (b)</div>

Figure 12: System (2) with parameters given in (3) and $\epsilon = 0.001$. (a) Successive local maxima in z (i.e. 'Lorenz plot') for $I = 3.25$. Since this Lorenz plot has not the classical shape of unimodal chaotic map, for these parameters, HR model does not exhibit chaotic motion, (b) Larger Lyapunov exponent for $I \in [3; 3.5]$. Obviously, for $I \approx 3.25$, the larger Lyapunov exponent is close to zero.
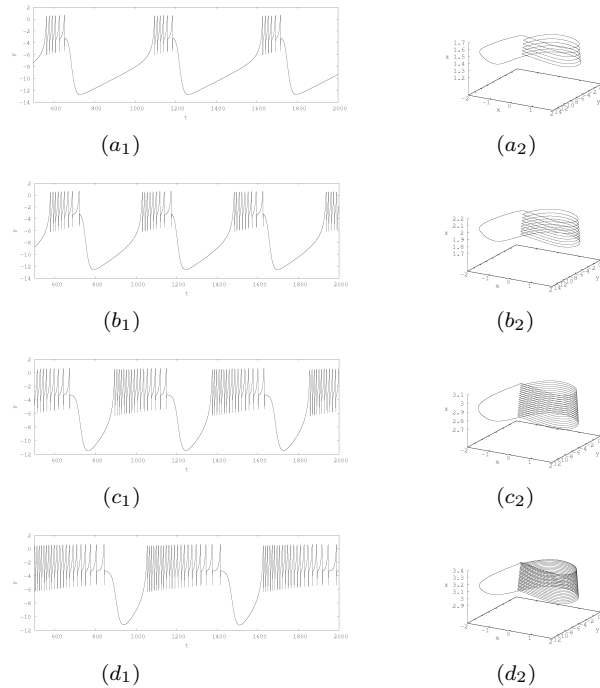
(a_1) (a_2)

(b_1) (b_2)

(c_1) (c_2)

(d_1) (d_2)

Figure 13: Time series and (x, y, z) phase portraits of system (2) with parameters given in (3), $\epsilon = 0.001$ and (a_1, a_2) $I = 1.5$, (b_1, b_2) $I = 2$, (c_1, c_2) $I = 3$, (d_1, d_2) $I = 3.25$. The larger the injected current I is ($I \in [1.4; 3.25]$), the larger the number of spikes within a burst is.

4   Conclusion

In this paper, an accurate numerical analysis of the asymptotic dynamics of Hindmarsh-Rose model has been done. We have discussed the chaotic dynamics of this system by use of different nonlinear dynamics numerical tools such as bifurcation diagrams, Lorenz plots and Lyapunov exponents for different parameter ranges. Two of the HR parameters, ϵ the time scale ratio between fast and slow dynamics and I the applied current, have been chosen as bifurcation parameters due to their biological meaning. It is obvious that the slow-fast motions due to the small parameter ϵ makes the dynamics even more interesting.

5   References

[1] I. Belykh, E. Lange, M. Hasler , Synchronization of Bursting Neurons: What matters in the Network Topology, *Phy. Rev. Lett.94*, **18**, (2005) 188101.1-188101.4.

[2] N. Corson and M.A. Aziz-Alaoui, Complex emergent properties in synchronized

neuronal oscillations, *From System Complexity to Emergent Properties, Eds. M.A. Aziz-Alaoui and C. Bertelle, Understanding complex systems series, Springer*, to appear in 2009.

[3] J.P. Françoise, Oscillations en Biologie : Analyse qualitative et Modèles, Collection Mathématiques et Applications, SMAI Springer, 2005.

[4] J M. Ginoux, B. Rossetto, Slow manifold of a neuronal bursting model, *Emergent Properties in Natural and Artificial Dynamical Systems, Eds. M.A. Aziz-Alaoui and C. Bertelle, Understanding complex systems, Springer*, 2006, pp. 119-128.

[5] J.M. Gonzalez-Miranda, Complex bifurcation structures in the Hindmarsh-Rose neuron model, *Int. J. of Bifurcation and Chaos* **17, 9**, (2007) 3071-3083.

[6] J. Guckenheimer, J. Tien and A. Willms, Bifurcations in the fast dynamics of neurons: implications for bursting, Bursting, The Genesis of Rhythm in the Nervous System, Eds. Stephen Coombes and Paul C Bressloff, World Scientific, 2005, pp. 89-122.

[7] B. Hille, Ionic channels of excitable membranes, second edition, Sinauer associates inc., 1992.

[8] J.L. Hindmarsh, R.M. Rose, A model of the nerve impulse using two first-order differential equations, *Nature* **296**, (1982), 162-164.

[9] J.L. Hindmarsh, R.M. Rose, A model of neuronal bursting using three coupled first order differential equations, *Proc. R. Sc. Lond.* **B221**, (1984) 87-102.

[10] A. Hodgkin, A. Huxley, A quantitative description of membrane current and its application to conduction and excitation in nerve, *J. Physiol.* **117**, (1952) 500-544.

[11] G. Innocenti, A. Morelli, R. Genesio, A. Torcini, Dynamical phases of the Hindmarsh-Rose neuronal model : Studies of the transition from bursting to spiking chaos, *Chaos* **17, 043128**, (2007) 1-11.

[12] E.M. Izhikevich, Dynamical systems in neuroscience - The geometry of excitability and bursting, The MIT Press, 2007.

[13] A.L. Shilnikov, M.L. Kolomiets, Methods of the qualitative theory for the Hindmarsh-Rose model : a case study, *Tutorial. J. Bifurcations and Chaos* **18, 8**, (2007) 1-27.

[14] A. Vidal, Periodic orbits of tritrophic slow-fast system and double homoclinic bifurcations, *Discrete and Continuous Dynamical Systems - Series B, special volume*, (2007) 1021-1030.